ISSN 1063-7745, Crystallography Reports, 2020, Vol. 65, No. 6, pp. 1002–1007. © Pleiades Publishing, Inc., 2020.
Russian Text © The Author(s), 2020, published in Kristallografiya, 2020, Vol. 65, No. 6, pp. 960–965.

SURFACE AND THIN FILMS

Mechanical Properties of Diamond-Like Silicon–Carbon Films Doped with Vanadium

A. N. Vinogradov[a], I. G. Dyachkova[b,*], A. V. Mamontov[a], I. S. Monakhov[a,c], S. Y. Shahbazov[a], and M. L. Shupegin[a,d]

[a] *Research Institute of Advanced Materials and Technologies, Moscow, 105087 Russia*
[b] *Shubnikov Institute of Crystallography, Federal Scientific Research Centre "Crystallography and Photonics," Russian Academy of Sciences, Moscow, 119333 Russia*
[c] *National Research University "Higher School of Economics," Moscow, 101000 Russia*
[d] *National Research University "Moscow Power Engineering Institute," Moscow, 111250 Russia*
**e-mail: sig74@mail.ru*

Received July 8, 2019; revised June 5, 2020; accepted June 22, 2020

Abstract—The influence of doping with vanadium on the mechanical properties of nanocomposite films deposited on silicon substrates has been investigated. It is found that the material tested is more likely brittle rather than plastic and that the hardness and elastic modulus of an undoped film are somewhat higher than those of vanadium-doped ones. With an increase in the Poisson ratio from 0.2 to 0.3, the hardness H_{IT} of undoped sample increases by 14%, and the elastic modulus E_{IT} decreases by 3.5%. Doping films with vanadium leads to a monotonic decrease in the elastic modulus E_{IT}. The concentration dependence of microhardness H_{IT} is complex: its minimum is observed at 8.8 at % V. It is established that the parameter of relative elastic strain energy of samples under indentation under investigation (η_{IT}) depends only slightly on film's Poisson ratio.

DOI: 10.1134/S106377452006036X

INTRODUCTION

Nanocomposites based on diamond-like silicon–carbon films are promising materials for various-purpose functional coatings because their electrical and mechanical properties can be varied in a wide range by introducing various metals into films with concentrations ranging from zero to several tens of percent [1, 2].

It was found that an increase in the tungsten concentration to 35 at % in a nanocomposite film causes a monotonic increase in its nanohardness from 18 to 26 GPa and in the elastic modulus from 135 to 350 GPa [3, 4]. An increase in the molybdenum content in a film changes the mechanical properties nonmonotonically: a minimum at 8 at % Mo is observed in the concentration dependences of nanohardness and elastic modulus [4]. This character of the concentration dependences of Mo- and W-containing films can be explained by the significant difference in the sizes of nanoparticles of metal carbides (2.5 and 1 nm at a metal content of 20 at %, respectively) and the difference in the distances between them. The deterioration of mechanical properties of films with an increase in molybdenum content is explained by the fact that the influence of larger molybdenum carbide nanoparticles at large distances between them on the mechanical properties of nanocomposite is weaker than that for tungsten-doped films. A subsequent increase in the metal concentration in film enhances the influence of nanocrystalline phase on the mechanical properties.

Prospects for various technological applications of nanocomposite silicon–carbon films require additional study of their structures and properties. In contrast to molybdenum- and tungsten-doped films, the mechanical properties of vanadium-containing nanocomposites have been studied insufficiently. The purpose of this work was to determine the nanohardness and elastic modulus of vanadium-containing nanocomposite films.

EXPERIMENTAL

Mechanical tests were carried out on nanocomposite films based on pure polyphenylmethylsiloxane (PPMS) and diamond-like vanadium-doped silicon–carbon films. Films of metal-containing nanocomposites were grown by simultaneous deposition of carbon-containing matrices from plasma and magnetron sputtering of metals [5]. Silicon–carbon films were grown in plasma of PPMS polymers near the substrate surface. The starting material for forming a matrix was PPMS: a liquid organic silicon compound $(CH_3)_3SiO(CH_3C_6H_5SiO)_3Si(CH_3)_3$ with a boiling

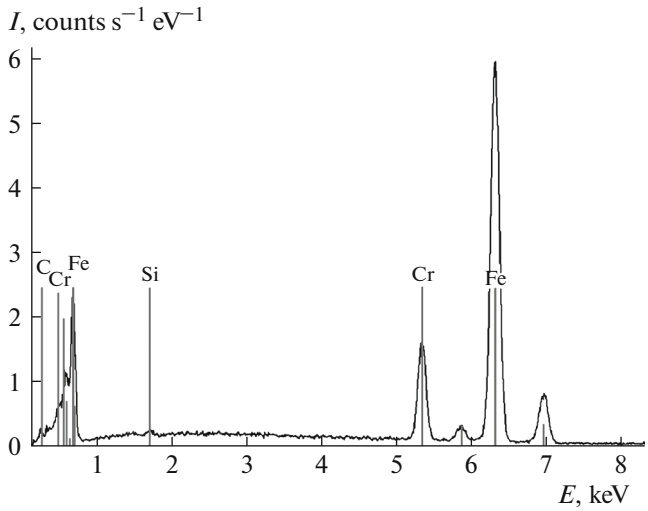

Fig. 1. Log of measuring the elemental composition of reference steel sample by X-ray fluorescence spectroscopy.

temperature in the range of 130–140°C. During film deposition, PPMS molecules in plasma form silicon–carbon polymers and then structure them on the substrate surface [6]. PPMS vapor feeding and vanadium sputtering were carried out simultaneously and independently. The metal-nanophase content was varied by locating substrates at different distances from the plasmatron and magnetron. The smaller the distance between the substrate and magnetron and the larger the distance between the substrate and plasmatron, the higher the metal concentration in the film was (and vice versa).

The metal content in the nanocomposites was determined by X-ray fluorescence spectroscopy. The measurements were carried out on a Lab Center XRF-1800 system [7]. Metal films were used as references in quantitative analysis. The elemental concentrations were calculated automatically using the system software. The film thickness was measured by a profilometer accurate to 0.01 μm.

Mechanical tests were performed on samples of nanocomposite films deposited on silicon substrates. Metal substrates were used as references to align the equipment. The elemental composition of the substrates was determined by X-ray fluorescence spectroscopy on a Lab Center XRF-1800 system (the measurement log for a steel sample (reference) is shown in Fig. 1).

The following samples of diamond-like films (DLFs) formed on 0.40-mm-thick silicon substrates were tested in order to determine the microhardness H_{IT} and elastic modulus E_{IT} (h is the film thickness):

(i) DLF50/1, DLF without metal doping, h = 2 μm;

(ii) DLF62/1, V-doped (9.8 at %) DLF, h = 4 μm;

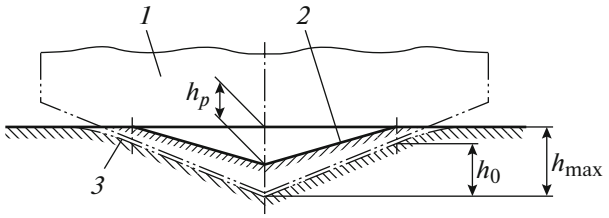

Fig. 2. Schematic diagram of the longitudinal cross section of the indentation zone: (*1*) indenter tip, (*2*) surface of the recovered impression in the sample after complete unloading, and (*3*) contact surface at h_{max} and F_{max}.

(iii) DLF64/1, V-doped (8.8 at %) DLF, h = 4.4 μm.

The tests were performed by instrumental indentation according to GOST (State Standard) R 8.748-2011 [8], taking into account ISO 14577-1:2002 [9]. A Shimadzu DUH-211S ultra micro hardness tester was used [10].

The tests were carried out under the following conditions:

(i) the indenter is a tetrahedral diamond Vickers pyramid;

(ii) the maximum penetration depth h_{max} is no more than 0.1h;

(iii) the maximum load F_{max} ranges from 5 to 20 mN (determined beforehand by the specified depth);

(iv) the test-cycle duration is from 25 to 45 s;

(v) the holding time under load is 10 s;

(vi) the number of tests for each sample ranges from 4 to 6;

(vii) the ambient temperature is 22–25°C;

(viii) the Oliver–Pharr calculation technique [11] is implemented in the DUH-S device software.

The DUH-211S resolution is:

(i) 0.2 μN (~0.02 mgf) for the force on the indenter, in the range of 0–1961 mN (0–200 gf);

(ii) 1 nm for the indenter run, in the range of 0–10 μm.

Figure 2 shows a schematic of the cross section of the sample and indenter in the zone of indentation by pyramidal Vickers tip [8, 9]. Here, h_P is the recovered-impression depth, h_{max} is the unrecovered-impression depth, and h_0 is the height of the contact zone with the recovered-impression diagonal.

Continuous indentation testing makes it possible to estimate microhardness based on not only residual plastic strain (as in the classical method, where recovered-impression diagonals are measured) but also taking into account the elastic properties of material.

The integral estimation of the ratio of elastic and plastic strains is carried out using work W_T on total displacements with an increase in the indentation load

and the reverse-run branch (describing the elastic force recovering the impression by work W_E). In this case, there are no external forces. It is known that the corresponding works can be determined by integrating the force functions over displacement:

$$W_T = \int_0^{h_{max}} F_1(h)dh, \quad W_E = -\int_{h_{max}}^{h} F_2(h)dh. \qquad (1)$$

Examples of dependences $F_1(h)$ and $F_2(h)$ are shown in Fig. 3a. Numerical integration methods implemented in the Shimadzu DUH-211S software were used in calculations. The ratio $\eta_{IT} = W_E/W_T$ characterizes the fraction of the work done on elastic displacements. In the indentation diagram, the work W_E is equal to the area under the curve $F_2(h)$ of the indenter reverse run, and the total work W_T of elastic and plastic strains is determined by the area under the curve $F_1(h)$. The work done on plastic strains $W_P = W_T - W_E$ is the area between the curves $F_1(h)$ and $F_2(h)$.

The microhardness, determined from the unrecovered impression of a Vickers pyramid (HV^*) under load, is related to the indentation hardness (H_{IT}) (in MPa) as $HV^* = 0.0945\ H_{IT}$ (kgf/mm^2).

RESULTS AND DISCUSSION

The results of the tests on determining the microhardness and elastic parameters of DLF films are presented in Table 1. One can see that the hardness and elastic modulus of the undoped film (DLF50/1) are much higher than those of vanadium-doped films.

The dependence of penetration depth h on indenter load F for one out of six tests of sample DLF50/1 is shown in Fig. 3a. The corresponding dependences for other samples have a similar shape.

The "loading–holding–unloading" cyclogram with a total duration of 28 s is shown in Fig. 3b (curve *1*). The phase of holding under constant load was about 10 s. The loading and unloading phases correspond to the linear portions in curve *1*, which indicates that the load was varied at a constant rate in the specified range of 0–5.1 mN.

The dependence of indenter penetration depth (run) on the test time with a stop for 10 s, at which relaxation could occur, is shown in Fig. 3b (curve *2*). However, no significant changes are observed in either load or depth.

Figure 4 shows the summary dependences of the main mechanical characteristics of DLFs on the vanadium concentration in them within the range of 0–9.8 at %. The dependences of elastic modulus E_{IT} and hardness H_{IT} are constructed for two Poisson ratios: $\nu = 0.2$ and 0.3. It can be seen in Fig. 4 that the film hardness begins to increase after 8.8 at % V, approaching the corresponding value for the film undoped with metal. The minimum manifesting itself in the film-hardness dependence on the V concentration (Fig. 4) is due to the combination of two competing factors: improvement of mechanical properties due to the increase in the carbide-phase content and simultaneous deterioration of mechanical properties of the silicon–carbon matrix because of the decrease in the carbon concentration.

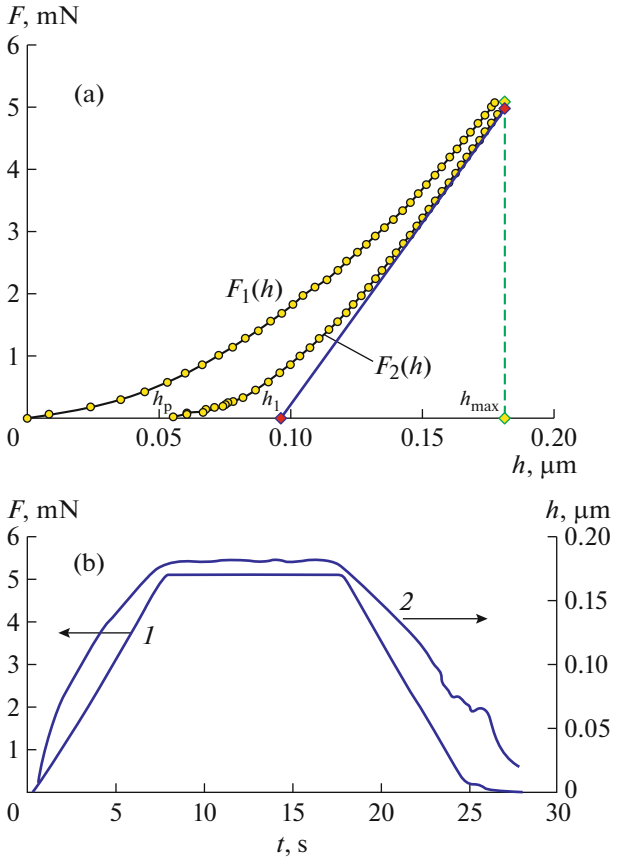

Fig. 3. (a) Indentation diagram for sample DLF50/1 and (b) dependences of the (*1*) load and (*2*) indenter-penetration depth on the indentation time.

Figure 5 shows the corresponding plots for the mechanical properties of reference steel sample in dependence of the maximum indenter load. The reference microhardness is about $H_{IT} = 10$ GPa ($HV^* = 945$ kgf/mm^2); it barely depends on the penetration force. With an increase in the load from 0.5 to 2 N, the relative fraction of elastic strain slightly increases from 35 to 39%, and the elastic modulus E_{IT} decreases by 30%. The classical value of the tensile modulus of this material (instrumental steel) is $E = 200$ GPa. In addition, one can see by this example that the E_{IT} value is 20% smaller than the nominal one. This problem is well-known [11]. Therefore, the results obtained for DLFs by this method can be used for comparative analysis. To determine the magnitudes of parameters,

Table 1. Main results of testing DLFs on a DUH-211S device

Characteristic	Sample		
	DLF50/1 no doping with metal	DLF64/1 8.8 at % V	DLF62/1 9.8 at % V
Film thickness, h, μm	2.0	4.4	4.0
Load, F_{max}, mN	5.09	19.74	18.65
Indentation depth, h_{max}, μm	0.185	0.405	0.387
	0.179	0.398	0.384
Indentation microhardness, H_{IT}, GPa (average values)	12.98	9.29	11.62
	14.87	9.69	11.86
Standard deviation, rms(H_{IT}), GPa	1.349		0.1953
	0.592	1.411	0.3427
Variation coefficient, VC = rms(H_{IT})/H_{IT} × 100 (%)	10.32		1.68
	3.983	14.56	2.89
Elasticity modulus under indentation, E_{IT}, GPa (average values)	97.56	82.05	76.41
	94.26	78.42	73.72
Standard deviation, rms(E_{IT}), GPa	3.687		1.014
	2.372	5.422	1.036
Variation coefficient, VC = rms(E_{IT})/E_{IT} × 100 (%)	3.780		1.328
	2.516	6.914	1.405
Reduced elasticity modulus, E^*, GPa	93.35	79.54	74.43
	95.00	80.15	75.66
Fraction of the work done on elastic strain, η_{IT}, %	69.99	64.02	68.19
	70.68	64.10	68.20
Diagonal of the pyramid cross section under load, $L_m = 7h_m$, μm	1.292		2.709
	1.253	2.835	2.687
Square-impression area, A, μm^2	0.285		1.333
	0.256	1.106	1.080

Here, $1/E^* = (1 - \nu^2)/E_{IT} + (1 - \nu_i^2)/E_i$; $E^* = 1/[(1 - \nu^2)/ E_{IT} + (1 - \nu_i^2)/E_i]$. For the DLF films, the Poisson ratios are $\nu = 0.2$ (upper value) and $\nu = 0.3$ (lower value). For the diamond indenter $\nu_i = 0.07$ and $E_i = 1.14 \times 10^6$ MPa. The substrate is a Si wafer with a thickness $h_0 = 0.40$ mm. The number of tests for each sample ranges from 6 to 11.

one must carry out more careful experiments with correction factors.

Figure 6 shows graphical dependences of the indenter load F on the penetration depth h for sample DLF64/1 for five experiments with specified maximum force F_{max} = 19.74 mN. It can be seen that the average maximum depth slightly exceeds 0.4 μm and the residual strain is about 0.15 μm, which corresponds to an impression diagonal of 1.05 μm.

In all diagrams obtained, the area corresponding to the elastic work is much larger than that for the plastic work. Therefore, the material tested is more likely brittle than plastic.

The indentation results for the material tested at specified Poisson ratios $\nu = 0.2$ and 0.3 did not show any significant difference. The values of hardness H_{IT} and elastic modulus E_{IT} differ by no more than 4%. At the same time, one can observe a stable regularity: at an increase in ν from 0.2 to 0.3, the hardness H_{IT} increases (e.g., from 11.6 to 11.8 GPa (by 1.9%) for sample DLF 62/1), while the elastic modulus E_{IT} decreases (from 76.4 to 73.7 GPa (by 3.64%)). The largest difference in the microhardness values (14.6%)

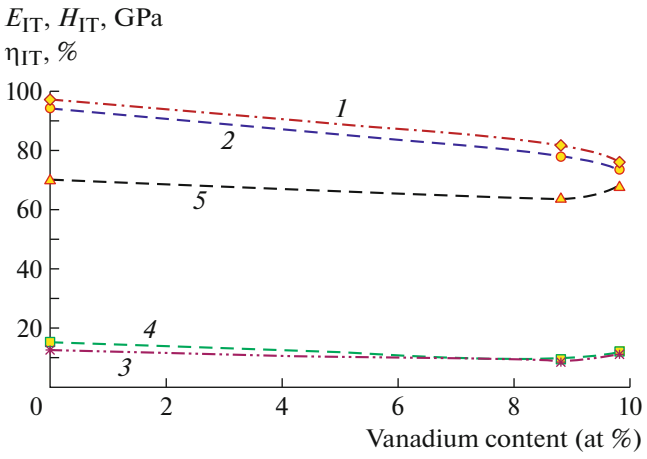

Fig. 4. Dependences of the following mechanical properties of the films doped with vanadium on its atomic content: elastic modulus E_{IT} (ν = (*1*) 0.2 and (*2*) 0.3), microhardness H_{IT} (ν = (*3*) 0.2 and (*4*) 0.3), and (*5*) fraction of the work done on elastic strain η_{IT} (W_E/W_T).

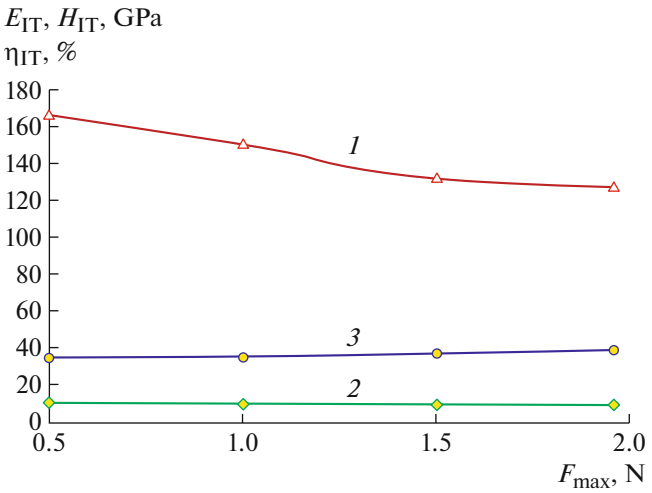

Fig. 5. Dependences of the following mechanical properties of the steel reference sample on the indentation force: (*1*) elastic modulus E_{IT}, (*2*) microhardness H_{IT}, and (*3*) fraction of the work done on elastic strain η_{IT} (W_E/W_T).

is observed for sample DLF50/1 (undoped with metal).

It should be noted that we compared the results of the tests in which the deviations from average values did not exceed 1.5 and 5% for E_{IT} and H_{IT}, respectively.

CONCLUSIONS

The results of determining the microhardness and elastic–plastic characteristics of the formed nanocomposite films showed that the material tested is more likely brittle than plastic: the fractions of the works of the elastic and plastic strains under indentation were 65–70 and ~30%, respectively. The indentation of material tested at a specified Poisson ratio ν showed that an increase in ν from 0.2 to 0.3 somewhat increases the hardness H_{IT} and decreases the elastic modulus E_{IT}. The changes in these characteristics do not exceed 4%.

It was established that the hardness and elastic modulus of sample DLF50/1 are much higher than those of vanadium-doped films. This fact is most likely due to the simultaneous occurrence of two competing processes in vanadium-containing films: increase in the values characterizing the mechanical properties of metal-containing films due to the increase in the carbide-phase content and deterioration of the mechanical properties of the second phase (silicon–carbon matrix), because carbon atoms are extracted from the matrix to form a metal carbide. Note that the contribution of nanoparticles to the mechanical properties of a nanocomposite is smaller than that of the matrix. However, a further increase in the metal content in the film enhances the influence of the nanocrystalline phase. A previous TEM study of vanadium-containing films revealed that the size of VC nanoclusters ranges from 1 to 2 nm at a vanadium concentration of 12 at % [12]. Apparently, carbide-phase clusters start to form at a V concentration of ~8.8 at %. It can be seen in Fig. 4 that the film hardness begins to increase at 8.8 at % V, approaching the corresponding value for the film undoped with metal. Thus, at a metal concentration of 8.8 at %, the carbide-nanophase contribution to the film mechanical properties becomes more significant than that of the silicon–carbon matrix. Note that the elastic modulus of the film monotonically decreased with an increase in the vanadium concentration; however, the fraction of the work done on elastic strains begins to increase at 8.8 at % V. One might suggest that the concentration dependence of the mechanical properties of vanadium-containing nanocomposite films is similar to that of molybdenum-containing films; therefore,

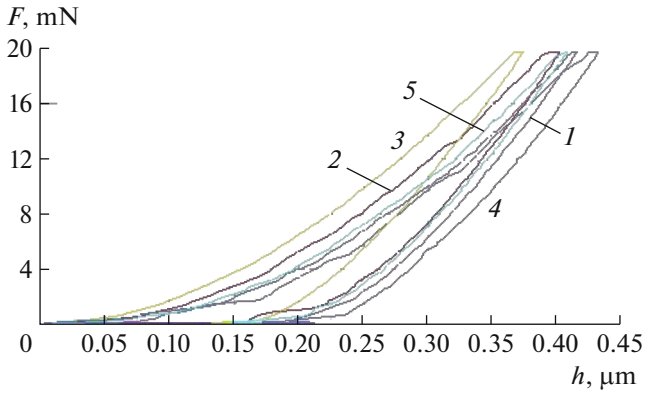

Fig. 6. Indentation diagrams of sample DLF64/1, obtained in five tests.

studies involving a large number of samples with different dopant concentrations should be performed.

FUNDING

This study was supported by the Ministry of Science and Higher Education of the Russian Federation within the State assignment for the Federal Scientific Research Centre "Crystallography and Photonics" of the Russian Academy of Sciences in the part concerning X-ray fluorescence spectroscopy and study of defects on the sample surface and by the State assignment of the Ministry of Science and Higher Education of the Russian Federation (project no. FNER-2019-0001) in the part concerning mechanical tests.

REFERENCES

1. M. S. Zibrov, Usp. Prikl. Fiz. **1** (2), 167 (2013).
2. M. Yu. Presnyakov, Ross. Nanotechnol. **9** (7–8), 59 (2014).
3. E. V. Zavedeev, O. S. Zilova, M. L. Shupegin, et al., Appl. Phys. A **122** (11), 1 (2016).
4. A. D. Barinov, A. I. Popov, and M. Yu. Presnyakov, Inorg. Mater. **53** (7), 690 (2017).
5. A. I. Popov and M. L. Shupegin, *Proc. V All-Russia School–Seminar of Students, Postgraduates, and Young Scientists in the Field of "Diagnostics of Nanomaterials and Nanostructures," Ryazan', RGRTU, 2012,* Vol. 2, p. 154.
6. A. D. Bozhko and M. L. Shupegin, *Proc. XI Int. Conf. "Radiation Physics of Solid State," Sevastopol', 2001,* p. 377.
7. http://www.shimadzu.com/an/elemental/wdxrf/-xrf1800/xrf.html.
8. GOST (State Standard) R 8.748–2011: Metals and Alloys. Measurements of Hardness and Other Characteristics of Materials under Instrumental Indentation, 2011.
9. ISO14577-1: Metallic Materials. Instrumented Indentation Test for Hardness and Materials Parameters.
10. DUH-211/DUH-211S User's Manual. Ultramicrotester Shimadzu for Dynamic Hardness Tests.
11. W. C. Oliver and G. M. Pharr, J. Mater. Res., No. 7(6), 1564 (1992).
12. O. M. Zhigalina, D. N. Khmelenin, S. M. Pimenov, et al., Crystallogr. Rep. **63** (5), 796 (2018).

Translated by Yu. Sin'kov